

Inconsistency of Force-Based Design Procedure

R.S.H. Smith¹ and W.K. Tso²

1. Yolles Partnership Inc., Toronto, Ont. Canada

2. Department of Civil Engineering, McMaster University, Hamilton, Ont. Canada,
email: tswok@mcmaster.ca

ABSTRACT: *The force-based seismic design procedure currently used assumes that the stiffness of the lateral force resisting elements is essentially independent of their strength. As a result, the period of the structure will remain the same as originally perceived, irrespective of how much the seismic base shear is reduced from the elastic strength. Current studies show that for a large class of reinforced concrete members such as piers, flexural walls and ductile moment resisting frames, their strength and stiffness are coupled. This leads to inconsistency between the assumed stiffness and the actual stiffness of the structure as designed. Using a wall structure as an example, this study examines the consequence of such inconsistency as it affects the estimation of ductility demand and seismic displacement of the structure, and points out the implication of continual use of the current force-based procedure. It is shown that the displacement-based procedure is a more simple approach to determine the seismic design strength of structures with stiffness-strength coupled elements.*

Keywords: R/C flexural walls; Coupled strength-stiffness relation; Force-displacement based design procedure

1. Introduction

The current force-based approach using an elastic design spectrum to obtain the seismic strength of a structure starts with an estimate of the lateral stiffness, or equivalently the period of the structure. Then, the elastic strength is obtained from the elastic design spectrum, based on the perceived period. The elastic strength is then modified by a reduction factor R to arrive at the design base shear. In this approach, it is assumed that the original stiffness estimate will not be affected when the design strength is reduced substantially from the elastic strength. Using an elasto-plastic representation as a first approximation, the behaviour of a family of similar structures designed using different R values would have force-displacement relations as shown in Figure (1a).

It has been pointed out [5] that one of the fallacies in the practice of seismic design is the assumption that the strength and stiffness of lateral force resisting members can be considered uncorrected. Extensive tests on reinforced concrete bridge piers showed that such an assumption is false. Studies on reinforced concrete flexural walls [3, 7] showed clearly that for a given steel yield strain, the yield curvature of a wall is a function of the wall length alone, and is insensitive to the amount of flexural reinforcement. Using elasto-plastic representation to describe the member behaviour, these members having

the same overall dimensions but different flexural reinforcement would have force-displacement relations as shown in Figure (1b). The member stiffness can be considered to be proportional to its yield strength, with the constant of proportionality being the yield displacement. Studies on flexural behaviour of beams [8] demonstrated that the assumption of independence between strength and stiffness is also inappropriate for ductile moment resisting concrete frames. It was noted that the structural stiffness of frames designed using the current force-based procedure is likely to be much lower than typically assumed by designers.

It becomes clear that for a large class of commonly used lateral force resisting elements, their strength and stiffness are coupled parameters. For a structure using such members as lateral force resisting elements, the stiffness, and also the period of the structure will therefore depend on its design strength. Since the design base shear of the structure is reduced from the elastic strength, the stiffness, or equivalently the period of the structure as designed will be changed from the original estimation. The objective of this paper is to examine the consequence of such inconsistency between the actual and perceived period of the structure using the current force-based design procedure. One consequence is that

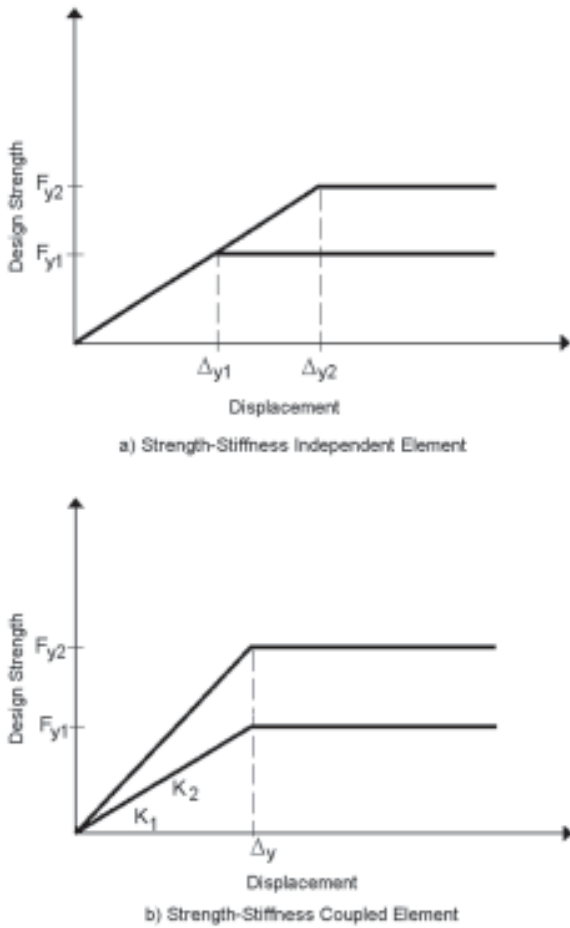


Figure 1. Force-displacement relationship.

the overall ductility demand is overestimated. Another consequence is that the seismic displacement will be underestimated. It is shown that since the yield displacement of the structure can be estimated beforehand, the direct displacement-based approach [6] can be used to advantage.

2. Force-Displacement Relations of Walls of Different Strength

To show the special strength and stiffness relationship of reinforced concrete walls, the moment-curvature relations of four geometrically identical walls are computed using the computer program RESPONSE [1]. In this program, a section analysis is carried out based on the concept of strain compatibility assuming a linear distribution of strain across the section. Each wall has an overall length $l_w = 3m$, thickness $b_w = 0.4m$ and height $h_w = 15m$, and contains one of four levels of concentrated end reinforcement as shown in Figure (2). The reinforcement ratios of these walls are 1.2%, 1.8%, 2.7% and 3.7% respectively. The concrete strength f'_c and modulus of elasticity are $35MPa$ and $28000MPa$ respectively, and the steel strength f_y and modulus of elasticity E_s are taken as $400MPa$ and $200000MPa$ respectively in the computation.

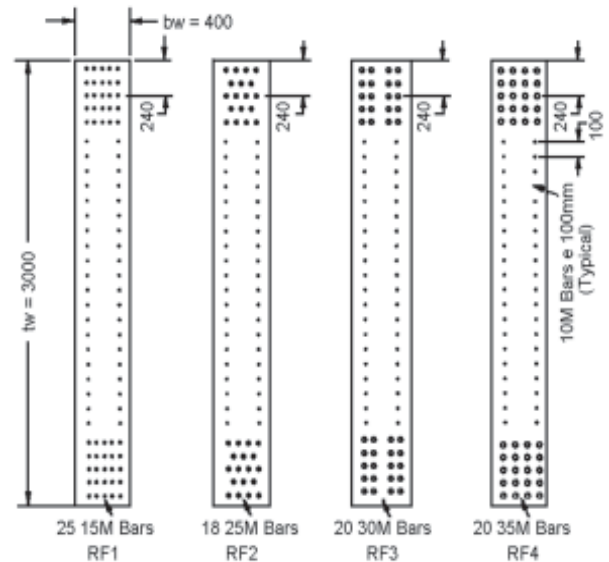


Figure 2. Reinforcement pattern for 3m long walls.

The results are presented in Figure (3a) showing that the four walls yield at approximately the same curvature. The yield curvature computed using the formula [3]

$$\phi_y = \frac{1.56f_y}{(E_s)(l_w)} \quad (1)$$

is also shown in the figure. It is evident that Eq. (1) provides a good estimation of the yield curvatures for the set of the walls considered, and the moment-curvature relation can be approximated as elasto-plastic. The force-displacement relations derived from the principles of structural mechanics are shown in Figure (3b). The relations remain elasto-plastic, with the yield displacement δ_y given by

$$(2)$$

Using Eq. (2), the 3m long and 15m high wall elements will have a yield displacement equal to $0.078m$. The yield strength F_y and the stiffness K are related as

$$F_y = \delta_y K = 0.078K \quad (3)$$

3. Determination of Elastic Strength

A simple structural model is chosen to illustrate the inconsistency of the current force-based design. The model consists of a top mass $m = 1296Mg$, supported by three equal massless parallel walls. Each wall has a length $= 3m$, thickness $b_w = 0.4m$, and height, $h_w = 15m$. It is assumed that the walls are well detailed such that shear and buckling failures will not occur, and the shear deformation and $P-\Delta$ effect are negligible. Only flexural

response of the walls, as represented in Figure (3b), is considered.

The design procedure follows the Uniform Building Code (UBC -1997) guideline for seismic zone 3 rock site requirement. For simplicity, the presentation is given assuming that the period of the model lies within the constant spectral velocity region of the UBC spectrum.

There are two approaches to arrive at the elastic strength of the structure that is strength-stiffness compatible.

3.1. The Iterative Approach

The iterative approach follows the traditional assumption that the system stiffness can be estimated based on the dimensions of the walls. Taking the effective moment of inertia of the set of walls $I_{eff} = 2.06m^4$, the system stiffness K is given by $K = 3EI_{eff} / h_w^3 = 51176kN/m$. This in turn gives the system period $T = 1.00s$. Within the period range of interest, the UBC design spectrum for zone 3 rock site is given by

$$F_e = mg \frac{C_v}{T} \tag{4}$$

where C_v is the seismic coefficient equal to 0.3 for the site considered. Using Eq. (4), the elastic strength F_e equals

to $3815kN$. However, a yield strength of $3815kN$ would not be compatible to a system having a stiffness of $51176kN/m$, according to Eq. (3).

An iteration procedure is necessary to arrive at a feasible design where the system strength and stiffness are compatible. The steps of this iterative procedure are schematically represented in Figure (4). Starting with an initial estimation of the system stiffness K_1 , an initial period T_1 is calculated. For this period, the strength demand F_1 is determined using the design spectrum. The stiffness that is compatible with this value of design strength is $K_2 = F_1 / \Delta_y$, where Δ_y is the known yield displacement of the system. The stiffness approximation is then revised and the calculations repeated. After several iterations, convergence on the elastic period and the elastic strength (F_e) will occur. Table (1) gives some sample calculations using this iterative procedure to obtain the elastic strength of the structural model with $3m$ long walls. The design parameters eventually converge to an elastic strength $F_e = 3645kN$ with a compatible period $T_e = 1.05s$. and stiffness $K_e = 46738kN/m$.

3.2. The Integrated Approach

The integrated approach incorporates the strength and stiffness characteristics of the elements directly in the design process. Expressing the system stiffness K by the system period T , Eq. (3) can be re-written as

$$F_y = 4\pi^2 \frac{\delta_y}{T^2} \tag{5}$$

Plotting Eq. (5) in the yield strength-period space gives the locus of feasible design solutions for the $3m$ long and $15m$ high walls system. Superimposing the UBC design spectrum on the same plot, the intersection of the two curves will simultaneously give the elastic strength F_e , and the system period, T_e as shown in Figure (5).

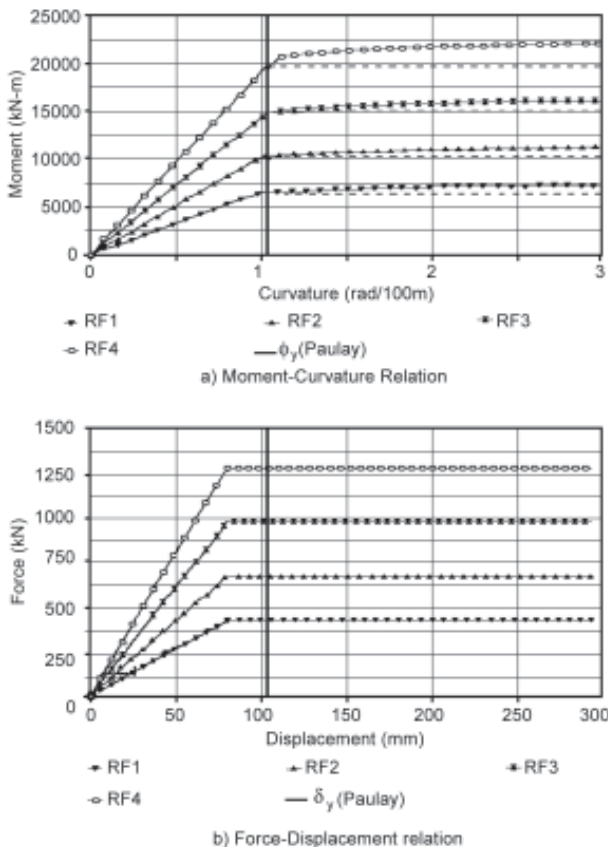


Figure 3. Deformation characteristics of 3m walls.

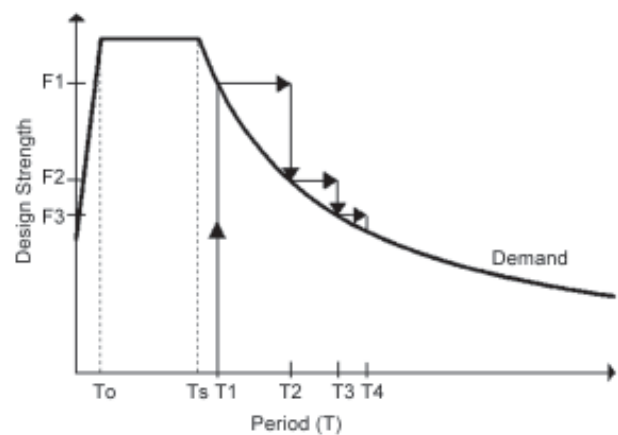
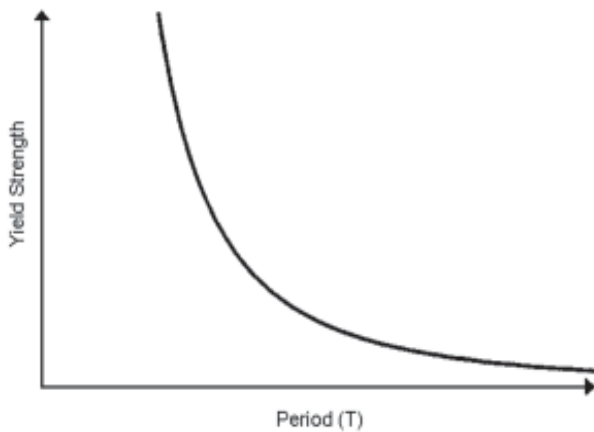


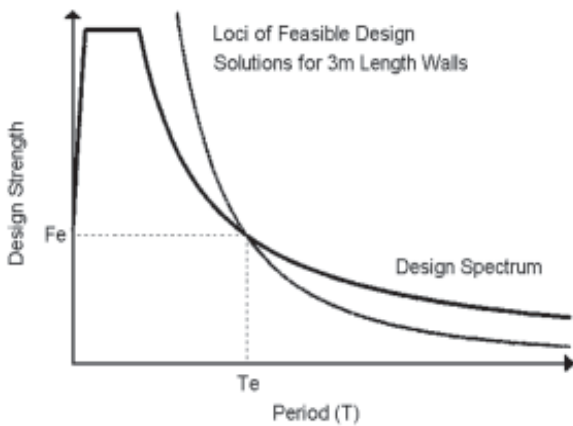
Figure 4. Schematic representation of the iterative approach.

Table 1. Iterative approach to determine elastic base shear.

K (kN/m)	T (sec.)	S _a (g)	F (kN)
51176	1.000	0.300	3815
48905	1.023	0.293	3729
47807	1.035	0.290	3687
47268	1.040	0.288	3666
47000	1.043	0.288	3656
46867	1.045	0.287	3650
46801	1.046	0.287	3648
46768	1.046	0.287	3647
46751	1.046	0.287	3646
46743	1.046	0.287	3646
46739	1.046	0.287	3645



a) Loci of Feasible Design Solutions for 3m Length Walls



b) Design Graph for Elastic Strength Determination

Figure 5. Integrated approach to determine elastic strength.

The intersection of the curves can be obtained analytically. Based on the elastic spectrum, the elastic strength is the yield strength. Equating Eqs. (4) and (5), the elastic period T_e is obtained

$$T_e = 4\pi^2 \frac{\delta_y}{g C_v} \tag{6}$$

Substituting the yield displacement of the wall system into Eq. (6) leads directly to the elastic period $T_e = 1.05s$. Once T_e is known, the elastic strength equal to 3645kN can be determined using Eq. (4). The advantage of using the integrated approach is that the elastic strength can be obtained directly and no iteration is necessary.

4. Determination of Design Base Shear

The design base shear is usually a fraction of the elastic strength. This reduction is accomplished by dividing the elastic strength by a force reduction factor R . For a system where its strength and stiffness are coupled parameters, a reduction in design strength from elastic strength would lead to a corresponding reduction in stiffness. This would in turn increase the period of the system. In the descending portion of the *UBC* spectrum, this period lengthening reduced the expected seismic demand. Therefore, the actual elastic demand to design base shear ratio will be less than R as originally envisioned.

This relationship is graphically illustrated in Figure (6a) where the subscript “e” defines the elastic design parameters where the elastic strength is based, and the superscript “*” defines the strength reduced design parameters for a given load reduction factor R .

The period of the strength reduced system T^* can be determined by expressing and the elastic period in terms of the corresponding system stiffness K^* and respectively. This in turn leads to a relation between T^* and given by

$$T^* = \sqrt{\frac{K_e}{K^*}} T_e = \sqrt{R} T_e \tag{7}$$

The design base shear (F^*) corresponding to a load reduction factor of R , is

$$F^* = \frac{F_e}{R} = mg \frac{C_v}{R_e} T_e \tag{8}$$

This is represented by point *b* in Figure (6a). The elastic demand for a system with period T^* , represented by point *c* in the same figure, is given by

$$F(T^*) = mg \frac{C_v}{R} \tag{9}$$

Using Eqs. (7), (8) and (9), the effective reduction factor (R_{eff}) is found to be

$$R_{eff} = \frac{F(T^*)}{F^*} = \sqrt{R} \quad (10)$$

As an example, consider the *SDOF* wall model described previously having an elastic strength $F_e = 3645kN$, a corresponding period $T_e = 1.05s$, and a stiffness $K_e = 46738kN/m$. Using a load reduction factor $R = 4$, the design base shear $F^* = 911kN$ and the system stiffness K^* is also reduced to $K^* = K_e/4 = 11684kN/m$. The corresponding period T^* is elongated to $(\sqrt{4})(1.05)$ or 2.10 seconds and the elastic demand for a system having a period of 2.1 seconds is 1825kN, according to the *UBC* spectrum. Therefore, the elastic demand to actual design base shear ratio is $R_{eff} = 1825/911 \approx 2$. This is consistent with the prediction using Eq. (10).

For medium period structures, the overall ductility demand can be estimated using the relationship equal to the force reduction factor. Since the real force reduction factor is equal to $R^{1/2}$, one should use the following relation to estimate the overall ductility demand of the structure

$$(11)$$

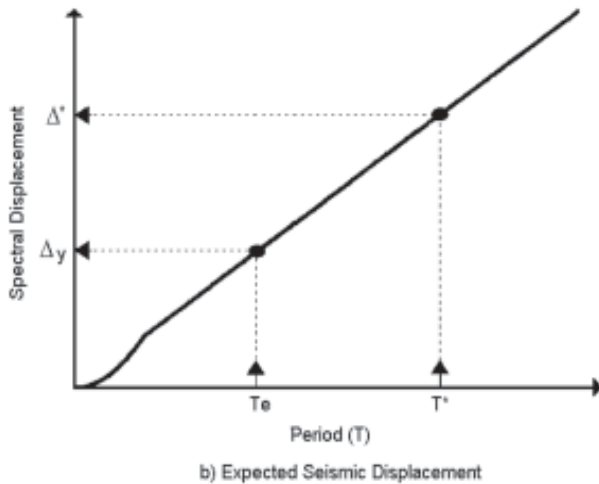
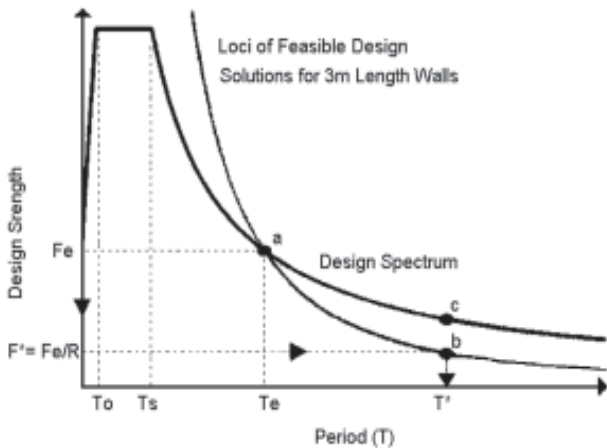


Figure 6. Effect of strength reduced design.

Continuing with the example, the design strength of 911kN is obtained using a force reduction factor $R = 4$. Using the traditional relation $\mu = R$, one would predict the ductility demand on the system would be 4. However, using Eq. (11), the ductility demand should be 2. As a result, the traditional way to estimate the ductility demand is over conservative.

To confirm the validity of Eq. (11), four *SDOF* wall systems were designed using load reduction factors R equals to 1, 2, 3, and 4. Four original earthquake time history records were used as seeds to generate four spectrum compatible records as excitation inputs as shown in Figure (7). Approximating the force-displacement curves of these models as elasto-plastic and assuming 5% viscous damping, the responses of these models subjected to the four time histories were computed. The mean ductility demands are plotted against the reduction factor R . The dispersion of the response is represented by the bar charts to show the maximum and minimum ductility demands. Shown in the same plots is a curve representing the relationship R_{eff} . It is seen that this R_{eff} curve predicts the mean ductility demands well. Using the traditional $\mu = R$ relation would grossly overestimate the ductility demand.

A second important consequence due to period changes is the change in seismic displacement. The maximum displacement of the strength reduced system should be approximately equal to the maximum elastic displacement of a system with the same period. Since $T^* > T_e$, the reduced strength system will therefore have a larger displacement than the displacement computed using the elastic period T_e . This relationship is represented in Figure (6b) where the *UBC* displacement spectrum is shown. The seismic displacement of a system having elastic period T_e, Δ_e , and that of the strength reduced system Δ^* can be written as

$$\text{and } \Delta^* = g C_v \frac{T^*}{4\pi^2} \quad (12)$$

Therefore, the seismic displacement Δ^* of the strength reduced system is given by

$$\Delta^* = \frac{T^*}{T_e} \delta_e = \sqrt{R} \delta_e \quad (13)$$

The significance of Eq. (13) can best be appreciated by referring to the example where the structural model is designed using $R = 4$. If the seismic displacement of that model is estimated based on the traditionally perceived design period equal to T_e , the estimate would be in error in as much as 100%, on the non-conservative side.

In summary, there are two consequences by not recognising that the stiffness and strength of the lateral force resisting elements are coupled parameters. First, the

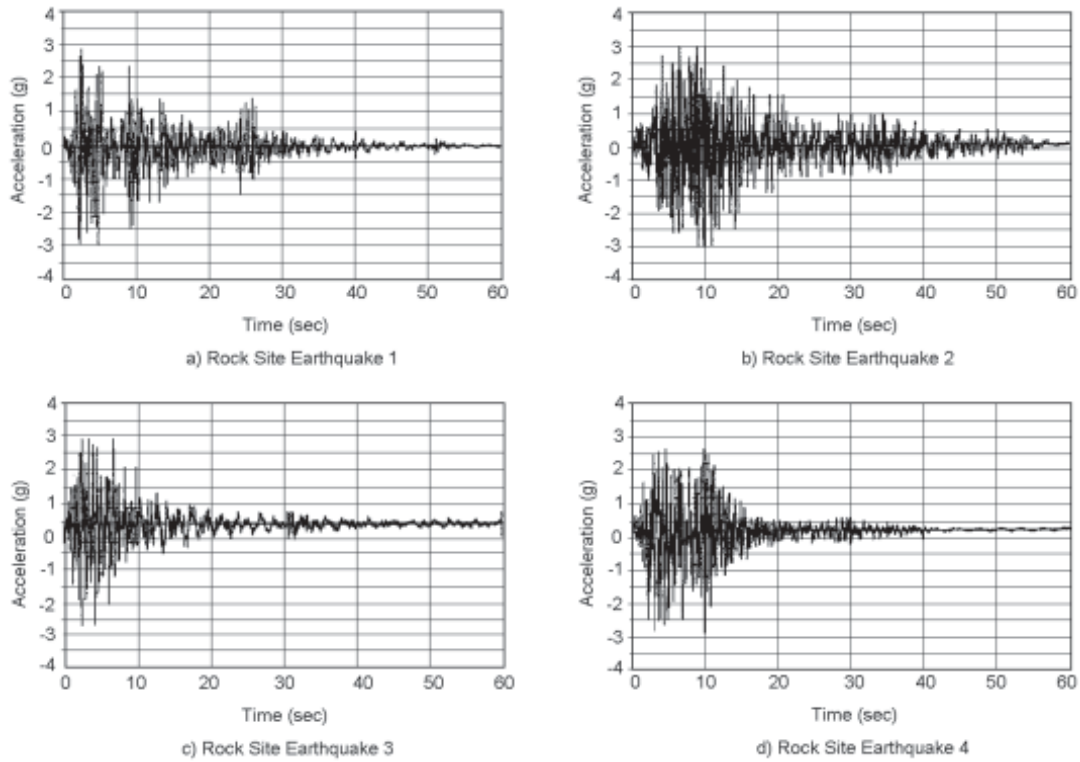


Figure 7. Four rock site spectrum compatible time-history records.

ductility demand for the structure will be overestimated. Eq. (11) can be used to give a more realistic ductility demand estimate. Second, the seismic displacement of the structure will be underestimated by a factor of $R^{1/2}$. The combined effect of overestimating ductility demand and underestimating of seismic displacement is that many reinforced concrete structures designed using the current force-based procedure will not reach their ductility capacity before the codified drift limit is reached. Specific examples of this situation have been noted in reference to the New Zealand code [7].

5. Displacement-Based Design Methodology

The previous section outlines the modifications needed to arrive at the strength reduced system design parameters F^* , T^* and K^* using the force-based design methodology. The same result can be obtained in a more direct manner using the displacement-based approach [2, 6]. In this approach, a target displacement needs to be defined. This target displacement may be selected based on a ductility capacity consideration such that

$$(14)$$

where μ is the design ductility and Δ_y is the effective yield displacement of the system. Once the target displacement has been defined, the design period for the system can be found from the design displacement

spectrum

$$(15)$$

The design stiffness K^* is then calculated based on

The design base shear F^* is then given by the equation

The previously described *SDOF* system will be used to illustrate the procedure. Assume that the system is to be designed and detailed to have a ductility capacity of 2. Then the target displacement should be $2\Delta_y = 0.156m$. Using the displacement spectrum derived from the *UBC* design spectrum for a rock site, the target system period = 2.10s. Accordingly, the design system stiffness = 11684 kN/m and the design strength is 911kN. This is identical to the design strength if a force-based design approach is used for a system with a load reduction factor of $R = 4$.

6. Drift-Based Target Displacement

The target displacement may be chosen based on drift-control in order to limit non-structural damages. In the performance-based design methodology, different performance levels are defined for the structure based on drift limits [9]. At the Operational Level of performance, the storey drift ratio limit is 0.5%. At the Life-Safety Level of performance, the storey drift ratio should not

exceed 1.5%.

The aspect ratio of the wall elements can be a useful parameter to determine whether the choice of the target displacement should be based on ductility capacity limit or drift limit. The drift angle $\theta \equiv \Delta_{top} / h_w$, represents the overall drift ratio of the structure. The drift angle at yield θ_y can be readily expressed as a function of the aspect ratio of the walls such that

$$(16)$$

When the ductility demand is μ , the seismic deflection will be and the drift angle becomes

$$(17)$$

Based on Eq. (17), a set of curves relating the drift angle to the aspect ratio of the walls can be created for different values of μ as shown in Figure (9a). A more useful plot for design purposes is to show the ductility associated with a particular level of drift as a function of the aspect ratio, shown in Figure (9b). It can be seen that for a wall with an aspect ratio that exceeds 4.8, the wall must remain elastic to satisfy the Operational Level drift limit. Ductility demand would no longer be the design criteria for such a wall. For walls with an aspect ratio greater than 7, the maximum ductility demand is less than or equal to 2 to satisfy the Live-Safety Level performance. Accepting the drift limits set by Vision 2000, it is likely that the design of many wall structures will be governed by the target displacement set by drift control consideration.

The advantage of using a displacement-based approach over the force-based approach to design wall structures becomes obvious. There is no need to perform a separate check on drift limitation in the displacement-based approach. Using design charts such as Figure (9), one can make the right choice to set the target displacement based on the smaller of (i) the displacement associated with the allowable drift ratio or (ii) the displacement associated with the maximum ductility demand.

7. Conclusions

Although the analysis was carried out on a structural model involving flexural walls, it is believed that the following conclusions are applicable to reinforced concrete structures having other types of lateral force resisting elements where their yield strength and stiffness are coupled. A table summarizing the coefficients to compute the nominal yield curvature for sections of different geometry in either concrete or steel is available [4].

- ❖ The traditional steps to obtain the elastic strength of a structure under force-based seismic design need to be modified so that the resulting strength and stiffness of the structure are compatible and reflect the realistic strength-stiffness characteristics of the elements used. The proposed integrated approach that determines both the elastic strength and period of the structure simultaneously is a viable alternative.
- ❖ Using a reduction factor R to obtain the design base shear from the elastic strength, the structure is actually more flexible than originally estimated. In other words, the structure as designed has a longer period than originally perceived.

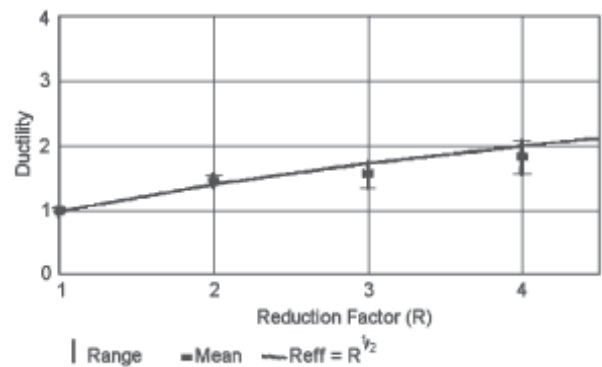


Figure 8. Comparison of actual and predicted ductility demands.

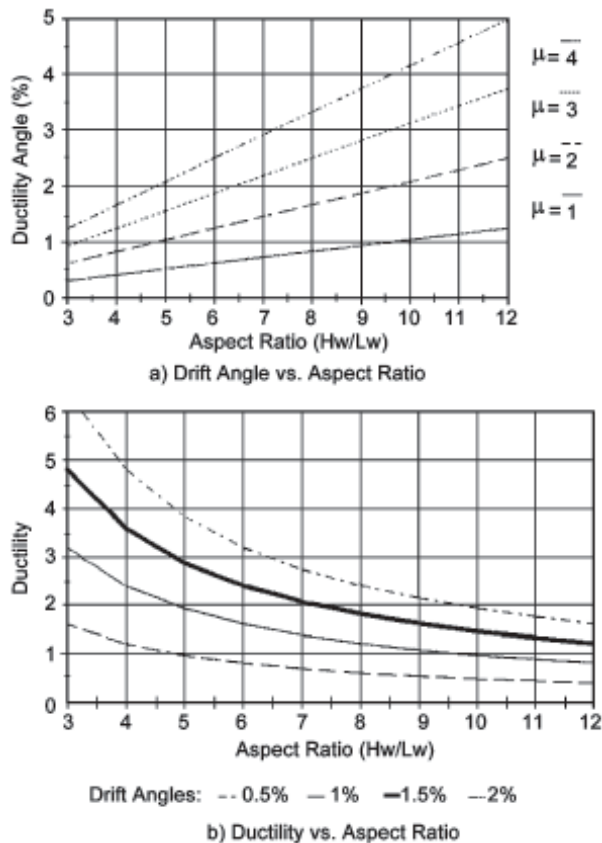


Figure 9. Drift angle/ductility-aspect ratio relationship.

- ❖ There are two consequences of the period change. First, the elastic strength demand on the structure is reduced. Therefore, even if the perceived force reduction factor is R , the effective reduction factor is less than R . For medium period structures, the effective reduction factor is equal to $R^{1/2}$. The ductility demand on the actual structure should therefore be estimated using the relationship $R^{1/2}$. Using the traditional formula would overestimate the ductility demand on the structure.
- ❖ The second consequence of period change is that the actual seismic displacement would be more than traditionally estimated. For medium period structures, the seismic displacement of the strength reduced structural system is $R^{1/2}$ times that determined based on the perceived design period. Therefore, the traditional way would underestimate the seismic displacement of the structure as designed.
- ❖ The design implication of conclusions 3 and 4 is that continual use of the current force-based design procedure would result in many reinforced concrete structures in which their ductility capacity may not be reached before they have violated the drift limits set for operational and non-structural element protection. Recognising the coupled nature between stiffness and strength of the lateral force resisting elements, and accepting the different drift limits set by Vision 2000, it is likely that the drift rather than the ductility capacity will govern the design decisions for many structures.
- ❖ Because the yield displacement of the structure can be established independent of the design strength, the displacement-based approach can be used to advantage to obtain the design base shear.

Acknowledgment

The authors wish to acknowledge the support from the Natural Sciences and Engineering Research Council of Canada (NSERC) for the work presented herein.

References

1. Collins, M.P. and Mitchell, D. (1990). "RESPONSE Version 1.0- A Program to Determine the Moment-Curvature Response of a Reinforced Concrete Section Using Plane Strain and Strain Compatibility Theories", Dept. of Civil Engineering, University of Toronto.
2. Moehle, J.P. (1992). "Displacement-Based Design of RC Structures Subjected to Earthquakes", *Earthquake Spectra*, **8**(3), 403-428.
3. Paulay, T. (1997). "Seismic Torsional Effects of Ductile Structural Wall Systems", *Journal of Earthquake Engineering*, **1**(4), 721-745.
4. Paulay, T. (2002). "Displacement Limits for Ductile Systems", *Journal of Earthquake Engineering and Structural Dynamics*, **31**(2), 583-599.
5. Priestley, M.J.N. (1993). "Myths and Fallacies in Earthquake Engineering—Conflicts between Design and Reality", *Bulletin of the New Zealand National Society for Earthquake Engineering*, **26**(3), 329-341, This Paper is reprinted in *Concrete International*, **19**(2), 1997, 54-63.
6. Priestley, M.J.N. and Calvi, G.M. (1997). "Concepts and Procedures for Direct Displacement Based Design and Assessment", *Proc. International Conference on Seismic Design Methodologies for the Next Generation of Codes*, Fajfar P. and Krawinkler H. Editor, A.A. Balkema, Rotterdam, 171-182.
7. Priestley, M.J.N. and Kowalsky, M.J. (1998). "Aspects of Drift and Ductility Capacity of Rectangular Cantilever Structural Walls", *Bulletin of the New Zealand National Society for Earthquake Engineering*, **31**(2), 73-85.
8. Priestley, M.J.M. (1998). "Brief Comments on Elastic Flexibility of Reinforced Concrete Frames and Significance to Seismic Design", *Bulletin of the New Zealand National Society for Earthquake Engineering*, **31**(4), 246-259.
9. SEAOC (1995). "VISION 2000: Performance Based Seismic Engineering of Buildings", *Structural Engineering Association of California*, Sacramento, California.
10. UBC (1997). "Uniform Building Code Volume 2: Structural Engineering Design Provisions", *International Conference of Building Officials*, Whittier, California.